

**SIMULATION ON THE COMBUSTION IN THE RACEWAY ZONE  
OF COREX MELTER GASIFIER**

*Ye SUN<sup>1,2</sup>, Ren CHEN<sup>1,2</sup>, Zuoliang ZHANG<sup>\*1,2</sup>, Guoxi WU<sup>1,2</sup>, Huishu ZHANG<sup>1,2</sup>,*

*Lingling LI<sup>1,2</sup>, Yan LIU<sup>1,2</sup>, Xiaoliang LI<sup>1,2</sup>, Yan HUANG<sup>1,2</sup>*

<sup>\*1</sup> Liaoning Key Laboratory of Optimization and Utilization of Non-associated Low-grade Iron Ore,  
Liaoning Institute of Science and Technology, Benxi 117004, China

<sup>2</sup> School of Metallurgy Engineering, Liaoning Institute of Science and Technology, Benxi 117004,  
China

\* Corresponding author: Zuoliang ZHANG; E-mail: zhang231167@lnist.edu.cn

*Two dimensional numerical simulation of the particle motion and combustion behavior in the raceway has been done to analyze the gas flow field, pressure field, temperature field, distribution of gas composition, as well as the effect of coke mass flow rate and blowing gas temperature on the maximum temperature in the raceway zone. The results show that the temperature in the cavity reaches the maximum in the upper part of the cavity region, and the maximum value is above 3000 K. During the combustion process, the concentration of O<sub>2</sub> decreases, and the concentration of CO increases. The highest CO content in the gas leaving the raceway zone and entering the coke bed is about 0.95, while the lowest O<sub>2</sub> content is 0.05.*

*Key words: COREX process; raceway zone; combustion; numerical simulation*

## **1. Introduction**

COREX is the world's first commercially established and industrially proven smelting-reduction process [1,2]. It is a two-stage process that involves pre-reduction in a shaft furnace, followed by final reduction and separation in a melter gasifier [3-5]. The melter gasifier is the key reactor of COREX process. Lateral injection of high speed gas into the packed bed in melter gasifier can cause the formation of granular circulation regions within the bed. These are commonly called 'raceways' due to the distinct shape of the path taken by entrained particles within the bed [6,7]. The raceway zone plays an important role in the smelting process of the COREX melter gasifier. A series of physical and chemical processes such as the shape and size of the raceway zone and the combustion reaction of coke determine the distribution of gas in the melter gasifier and provide a source of heat for the reduction of iron oxide. It is also an important basis for the smoothness of the furnace. Therefore, the research on the raceway zone of the corex melter gasifier has important theoretical and practical significance. In the numerical simulation of coke particles in the blast furnace and pulverized coal injection combustion, most of the research is carried out in one dimensional simulation and two dimensional simulation. A few researchers conducted gas-particle two-phase flow in the blast furnace straight blow pipe and the orbit of the

traditional pulverized coal particles injection gun in the blast furnace tuyere was simulated in three dimensions.

Guo considered the coke pyrolysis, combustion, gas turbulent chemical reaction and other processes in the raceway zone [8]. Using CFX, a physical model based on particle orbit was established and carried out a numerical simulation for the model. Qiu et al. studied the combustion process of oxygen-coal burner in the raceway before blast furnace tuyere injected into pulverized coal, conducted a computer simulation for the combustion process of oxygen-coal burners based on different quantity of pulverized coal and oxygen concentration [9]. Zhang et al. established a three dimensional mathematical model of turbulent gas-solid two-phase flow and pulverized coal combustion in the raceway zone of the blast furnace based on the Euler gas phase equation and the Euler particle continuous equation, the momentum equation and the equation of Lagrange energy and mass change [10]. Zhang et al. used FLUENT commercial software, through PDF to define fuel composition, gas phase turbulent flow using standard k- $\epsilon$  model, the particle phase adopts the random orbit model, the differential equation is discretized by the finite difference method and the SIMPLE algorithm is used for the governing equation [11]. The pulverized coal combustion simulation was performed on the columnar combustion furnace. Gu studied the aerodynamic characteristics and pulverized coal combustion process in the blast furnace tuyere using a three-dimensional steady-state two-phase flow and multi-fluid mathematical model of chemical reaction based on the Eulerian coordinate system [12]. The two-fluid model was used to establish the combustion model of pulverized coal in the tuyere. The effects of pulverized coal combustion characteristics, spray angle and particle diameter on the gas flow field distribution and combustion characteristics in the tuyere were investigated. Huang et al. used FLUENT software to determine the boundary of the raceway zone by the double Euler model, and then corrected the boundary of the raceway zone through the swirling zone and its surrounding combustion simulation [13]. Finally, the stable boundary was obtained and simulated the gas composition and temperature distribution bases on this model, and considering the combustion conditions under coal injection process. Shen et al. established a series CFD models to study the coal combustion in raceway zone [14,15]. Recently, the coupled CFD-DEM model was also developed to the particles and gas flow in the raceway in blast furnace [16-20].

Based on the previous work, this paper conducts a two-dimensional steady-state numerical simulation of the combustion behavior of coke particles in the raceway zone and analyzes the effects of different physical properties and operating parameters on the temperature field of the raceway zone. In the simulation process, the component transport equation, the discrete phase model (DPM), k- $\epsilon$  turbulence models, P1 radiation models and porous media models are mainly adopted.

## **2. Governing equation**

### **2.1. Basic control equation of fluid phase**

#### *2.1.1 Mass conservation equation*

The mass conservation equation is also called the continuous equation. Any flow must meet the law of conservation of mass. The law can be expressed as: the increase of mass in the fluid micro-body per unit time is equal to the net mass flowing into the micro-element during the same time interval. According to this law, the mass conservation equation is given by the equation:

$$\frac{\partial \rho}{\partial t} + \nabla \cdot (\rho \bar{v}) = S_m \quad (1)$$

Where,  $\rho$  is density;  $t$  is time;  $\bar{v}$  is the speed vector;  $S_m$  is the source term of mass and is equal to zero.

### 2.1.2 Momentum conservation equation

The momentum conservation equation is also the basic law that must be met by any flow system. The law can be expressed as: the change rate of the momentum of the fluid in the micro-body to time is equal to the sum of the forces acting on the micro-body. This law is actually another expression of Newton's second law. According to this law, the following equation can be obtained.

$$\frac{\partial}{\partial t} (\rho \bar{v}) + \nabla \cdot (\rho \bar{v} \bar{v}) = \nabla \cdot (\mu \text{grad} \bar{v}) + S_v \quad (2)$$

Where,  $S_v$  is the generalized source term of the momentum conservation equation. The momentum equation of the constant density and normal physical fluid motion is called the Navier-Stokes equation, also referred to as the N-S equation. The influence of coke porous media has been considered in this term, the equations are as follows.

$$S_v = 150 \cdot \frac{(1-\varepsilon)^2}{\varepsilon^3} \cdot \frac{\mu}{(\Phi d)^2} \cdot u + 1.75 \cdot \frac{(1-\varepsilon)}{\varepsilon^3} \cdot \rho \cdot u^2 \quad (3)$$

### 2.1.3 Energy conservation equation

The energy conservation equation is the basic law that must be met by a flow system containing heat exchange. The law can be expressed as: the rate of increase of energy in the micro-body is equal to the net heat flux into the micro-element plus the work done by the volume and surface forces on the micro-element. This law is the first law of thermodynamics.

The temperature  $T$  as a variable for the energy conservation equation can be expressed as follows.

$$\frac{\partial}{\partial t} (\rho C_p T) + \nabla \cdot (\rho \bar{u} C_p T) = \nabla \cdot (k \text{grad} C_p T) + S_T \quad (4)$$

Where,  $C_p$  is the specific heat capacity;  $T$  is temperature;  $k$  is heat transfer coefficient of the fluid;  $S_T$  is the internal heat source of the fluid and the part of the fluid energy converted into heat due to viscous action, and is equal to zero.

### 2.1.4 Component equation

In a particular system, each component must meet the law of components mass conservation due to the multiple chemical components. For a certain system, the conservation law of component mass can be expressed as: the rate of change of mass of a chemical component in a system to time is equal to the sum of the net diffusion flux through the system interface and the productivity of the component produced by the chemical reaction.

According to the law of components mass conservation, the component mass conservation equation of components  $S$  can be obtained is as follows.

$$\frac{\partial \rho Y_i}{\partial t} + \nabla \cdot (\rho \bar{v} Y_i) = \nabla \cdot (D_i \text{grad} \rho Y_i) + S_i \quad (5)$$

Where,  $Y_i$  is the volume concentration of component  $i$ ;  $\rho Y_i$  is the mass concentration of component  $i$ ;  $D_i$  is the diffusion coefficient of component  $i$ ;  $S_i$  is the mass of component  $i$  produced by a chemical reaction of per unit volume per unit time within the system. The term on the left and right of the above formulation are time accumulation term, convection term, diffusion term and reaction term respectively. The sum of the mass conservation equations of the components is the continuous equation of the system, is  $\sum S_i = 0$ . Therefore, if there is  $z$  components, then only  $z-1$  independent component mass conservation equation.

## 2.2. Basic control equation of particle phase

### 2.2.1 Particle balance

$$\frac{dv_p}{dt} = F_D (v - v_p) + \frac{g(\rho_p - \rho)}{\rho_p} + F \quad (6)$$

Where,  $F$  is the additional acceleration term,  $F_D (v - v_p)$  is the drag of a unit mass of particles, and

$$F_D = \frac{18\mu}{\rho_p d_p^2} \frac{C_D \text{Re}}{24} \quad (7)$$

Where,  $v$  is fluid phase velocity;  $v_p$  is particle speed;  $\mu$  is the molar viscosity of the fluid;  $\rho$  is the density of the fluid;  $\rho_p$  is the density of the particles;  $d_p$  is the particle diameter;  $C_D$  is the drag coefficient;  $\text{Re}$  is the relative Reynolds number, which is defined as

$$\text{Re} \equiv \frac{\rho d_p |v_p - v|}{\mu} \quad (8)$$

### 2.2.2 Particle surface reaction heat conservation equation

$$m_p c_p \frac{dT_p}{dt} = h A_p (T_\infty - T_p) - f_h \frac{dm_p}{dt} H_{\text{reaction}} + A_p \varepsilon_p \sigma (\theta_R^4 - T_p^4) \quad (9)$$

where,  $m_p$  is particle quality, kg;  $c_p$  is the specific heat capacity of the particles, J/(kg·K);  $A_p$  is particle surface area, m<sup>2</sup>;  $T_\infty$  is continuous phase temperature, K;  $h$  is convection heat transfer coefficient, W/(m<sup>2</sup>·K);  $\varepsilon_p$  is particle emissivity;  $\sigma$  is Steven-Boltzmann constant, 5.67×10<sup>-8</sup> W/(m<sup>2</sup>·K<sup>4</sup>);  $\theta_R$  is radiation temperature,  $\left(\frac{G}{4\sigma}\right)^{1/4}$ ;  $H_{\text{reaction}}$  is the heat generated by the surface reaction of the particles;  $f_h$  is the ratio of absorption heat of the particles accounts for the total reaction heat. When the carbon particle combustion product is CO, it is recommended to be 1.0 and the CO<sub>2</sub> is 0.3.

## 3. Model establishment and assumptions

The turbulence model and radiation model are  $k-\varepsilon$  model and P1 model respectively, the particle motion and combustion process uses the DPM combustion model and the porous medium model.

The mainly reaction of coke particles in the raceway zone as follows:



The kinetic constants of the above three reactions are shown in Tab. 1 [5].

**Tab. 1 Reaction kinetic constants**

Reaction	$K = B \exp\left(-\frac{E}{RT}\right)$	
	$B_i$ (m/s)	$E_i$ (J/mol)
$\text{C} + \text{O}_2 \rightarrow \text{CO}_2$	$1.225 \times 10^3$	$9.977 \times 10^4$
$2\text{C} + \text{O}_2 \rightarrow 2\text{CO}$	$1.813 \times 10^3$	$1.089 \times 10^5$
$\text{C} + \text{CO}_2 \rightarrow 2\text{CO}$	$7.351 \times 10^3$	$1.380 \times 10^5$

The whole calculation area is divided into a raceway zone cavity and a porous medium zone. As shown in Fig. 1, the calculation domain is determined according to the cross-sectional dimension of raceway zone in the COREX melter gasifier, and the whole area is rectangular area for  $4.69\text{m} \times 2.68\text{m}$ . The diameter of the tuyere is 30mm, the depth of the raceway is 1.4m, the height is 1.3m, and the porosity of the porous medium is 0.4. In this work, the average mesh size is 20 mm in the present simulation. They are mostly structured meshes. We did the sensitivity study of mesh size with average size of 80 mm, 60 mm, 40 mm, 20 mm and 10 mm. The difference of depth of the raceway between 40 mm and 20 mm is 3.1% while that between 20 mm and 10 mm is within 0.5%. This suggests that the mesh size of 20 mm is reasonable and confirms the mesh independence.

In the process of building the model, some simplifications and assumptions have been made to simplify the processing and reduce the complexity of the model, including the following.

(1) This paper mainly simulate the combustion process of coke particles in the raceway zone. The shape of the coke particles is assumed to be spherical, and the initial temperature of the coke from the raceway cavity boundary to the raceway zone with the gas flow is 1800 K.

(2) Only the coke combustion reaction is considered in the raceway zone, and the combustion product is co, regardless of the endothermic process in which the sponge iron is reduced. The porous medium region around the raceway region does not consider the carbon dissolution reaction.

(3) The non-elastic collision is adopted between the carbon particle and the boundary of the raceway. The tangential velocity and the normal velocity are both lost after the collision. The loss is achieved by assuming a loss coefficient with 0.3.

(4) In the fluent treatment, because the boundary of the raceway region cavity are added coke particles inconveniently, the coke particles enter into the raceway zone are added through the circumference along the edge of the raceway zone.

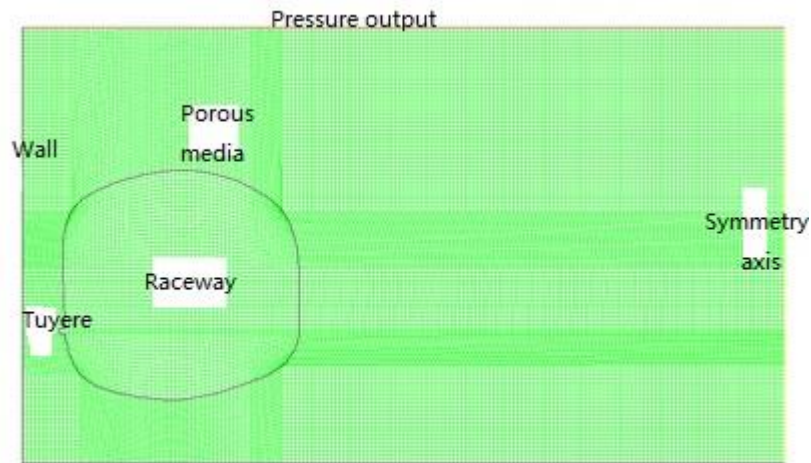


**Fig. 1** Schematic diagram of computational domain

In this simulation, a series of typical working conditions are used to analyze the flow field, pressure field, temperature and concentration field of the raceway zone. The main operating conditions and process parameters are shown in Tab. 2.

**Tab. 2 Parameters used in modeling**

Parameters	Parameter value	Unit
Particle diameter	200	$\mu\text{m}$
Particle flow rate	0.60	kg/s
Particle temperature	1800	K
Oxygen blowing speed	90	m/s
Oxygen temperature	1000	K
Tuyere diameter	30	mm
Coke bed voidage	0.4	-
Operating pressure	3.5-4.0	atm

#### 4. Simulation results analysis

##### 4.1. Analysis of combustion simulation results in the raceway zone

The simulation results and analysis are as follows.

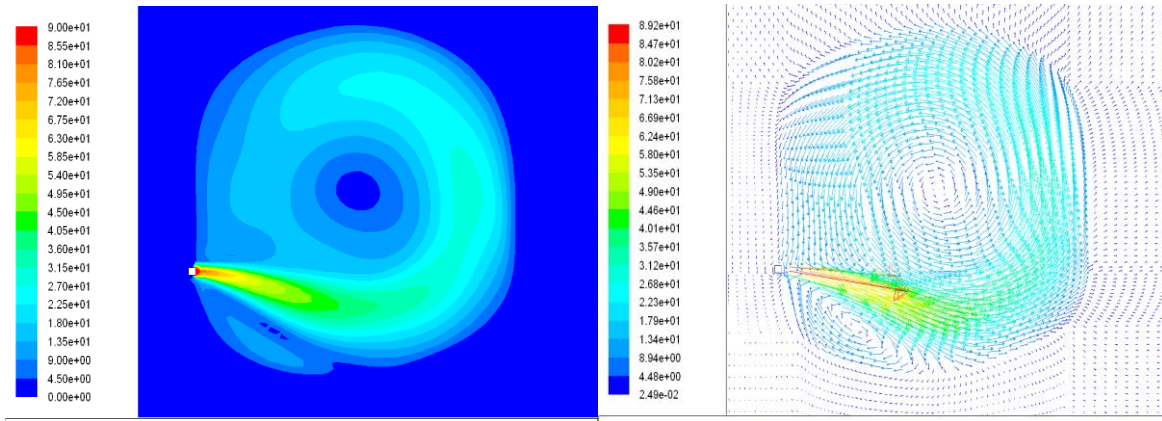


**Fig. 2** Contours of velocity

**Fig. 3** Velocity vectors

It can be seen from the contours of velocity that the airflow exhibits a state of swirling motion in the raceway zone (Fig. 2). First, the airflow is sprayed from the tuyere into the raceway zone cavity. At this time, the velocity is large and the resistance is small, and the gas moves forward straightly. When hitting the side wall of the cavity, entering into the area of the coke bed with porosity 0.4, the resistance increases sharply, but the resistance in the raceway zone cavity is relatively small, so that part of the airflow passes through the coke bed while the other part of the airflow moves along the boundary of the raceway cavity within the cavity. A ‘cavity’ appears in the center of the raceway cavity, where the velocity is almost zero which is agreement with the results of physical experiments. In addition, combined with the velocity vector diagram (Fig. 3), it can be seen that there is a small circulation in the lower part of the raceway zone cavity. Because that when the airflow of the tuyere sprays into the raceway, the airflow will develop to both sides, and the lower layer resistance is large, and the lower bed has high resistance and it is difficult for the airflow to develop downward. Therefore, the upper raceway zone is large and the lower raceway zone is small, which is also an important factor in the final shape of the raceway zone cavity.

The gas flows into the raceway zone cavity and reaction with the coke particles. After the reaction, the gas develops toward the coke layer. Because the resistance of the coke bed increases, the space also increases, thus the gas velocity becomes smaller and moves upward along the coke bed finally. It can be clearly seen in the contours of velocity and velocity vectors.

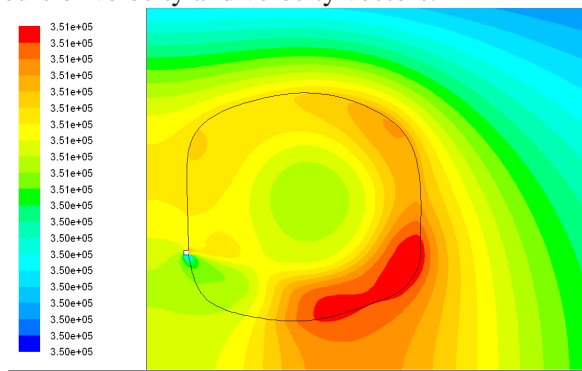


**Fig. 4** Contours of static pressure

Fig. 4 shows a contours of static pressure of the raceway zone and its vicinity. It can be seen from the figure that the pressure layering is obvious, the pressure is highest along the boundary of the raceway and its vicinity, and gradually decreases toward the surrounding. The pressure in the boundary region of the cavity facing the tuyere is the largest, because the gas injected at the tuyere is subjected to great

resistance, then the pressure is sharply increased. The obstructed airflow begins to move upward along the boundary of the raceway. During the upward motion, the airflow also spreads to the area of the coke bed, thus the pressure slowly decreases, but the pressure at the boundary of the raceway is still greater than the pressure in the surrounding area.

Along the edge of the raceway toward the inside of the cavity, the pressure value gradually decreases, and the pressure at the center of the cavity is the lowest. This situation is agreement with the velocity vectors of the raceway, where the velocity is almost zero. And along the edge of the raceway to the outer coke bed area, the pressure value also drops slowly with a certain gradient.

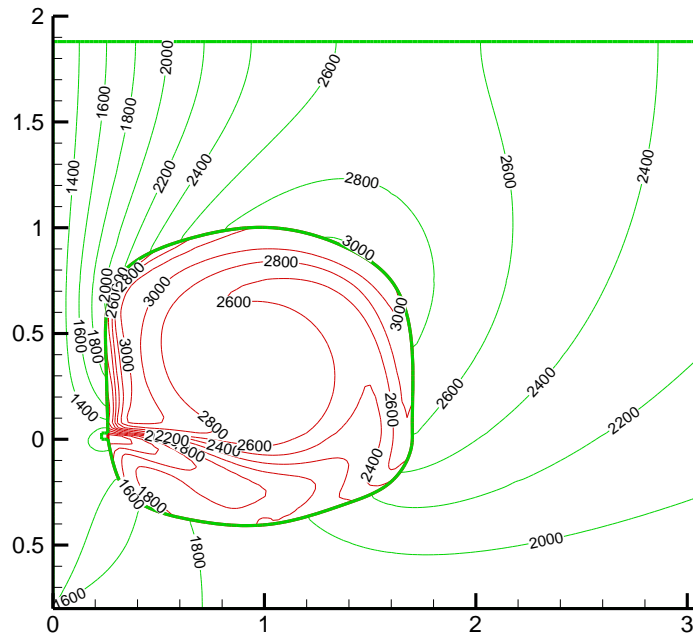


**Fig. 5** Temperature contour map of raceway zone

Fig. 5 shows the temperature contour map of raceway zone. It can be seen from the figure that the temperature at the tuyere is relatively low, and the temperature rises along the direction of the airflow upward, and the temperature can reach up to 3 000 K above at the upper edge of the raceway zone. Along the boundary of the raceway to the peripheral coke area, the temperature begins to decrease again.

The temperature of oxygen entering the tuyere is lower. At this time, the oxygen is rapidly injected, but it has not react with the coke particles, hence the temperature at the tuyere is low. As oxygen enters the raceway and begins to react with the coke particles to release a large amount of heat, the temperature of the gas stream begins to rise sharply. Continue along the boundary of the raceway zone, the coke is completely burned and the temperature is maximized. When the gas flow diffused from the raceway zone cavity to the coke bed area, the endothermic reaction of C and CO<sub>2</sub> in the coke bed was not considered in this study, but the endothermic and thermal properties of the porous media of the coke bed were also considered. Thus, as the distance from the raceway increases, the temperature begins to decrease gradually.

Figs.6 and 7 are O<sub>2</sub> and CO volume fraction distribution diagrams respectively. It can be seen from the O<sub>2</sub> and CO volume fraction distribution that the concentration of O<sub>2</sub> is the highest at the tuyere, while the concentration of CO is the lowest. As the tuyere advances further into the raceway zone, the combustion reaction commences, O<sub>2</sub> begins to be consumed, and carbon oxides begin to be produced (in this paper, the formation of CO is mainly considered). Combination with the temperature diagram, we can see the temperature starts to rise sharply. As the airflow continues to move upward, the



temperature reaches the highest value, the volume fraction of CO is getting higher and higher, and the volume fraction of CO reaches the highest value of above 0.95. At this time, O<sub>2</sub> is the lowest value of 0.05.

The coke bed area around the raceway zone that CO is the majority and O<sub>2</sub> is the minority, especially in the upper part of coke bed and in the radial direction of the hearth, the maximum CO can reach above 0.95, while the O<sub>2</sub> is less than 0.05. This is in agreement with the actual situation. Most of the O<sub>2</sub> is consumed in the cavity of the raceway zone, reacting with the coke particles to produce CO gas, and when entering the upper region of the coke bed area, CO has an absolute advantage substantially.

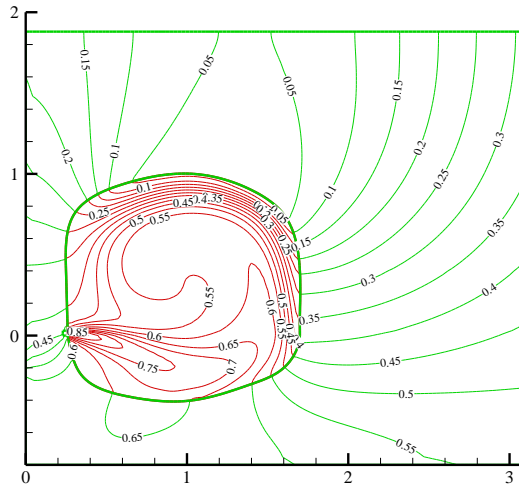


**Fig. 6** Volume fraction of O<sub>2</sub>

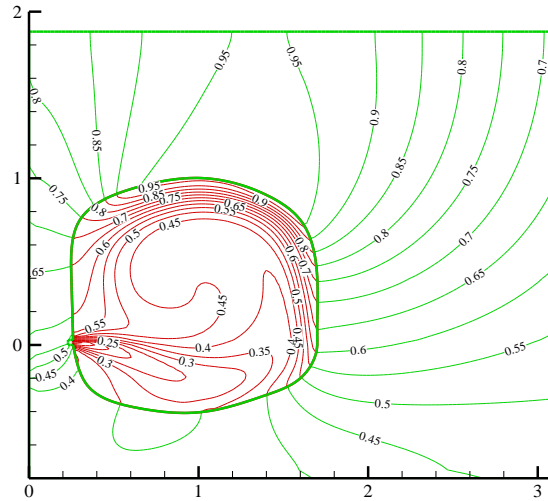


**Fig. 7** Volume fraction of CO

#### 4.2. Influence of particle flow rate on the maximum temperature of raceway zone

The particle flow rate is the total mass of coke particles that are entrained by the blowing gas from the boundary of the raceway zone per unit time, that is the maximum coke mass that can participate in the combustion reaction in the raceway zone. The velocity of the blowing gas refers to the velocity of oxygen injected into the raceway zone from the tuyere.

This section research the effects of particle injection flow rate on the maximum temperature of the raceway zone under different gas velocity. The blowing gas temperature is set to 1 000 K and the particle diameter is 100 μm.

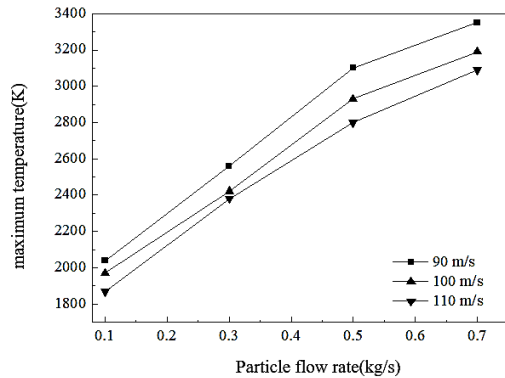


**Fig. 8** Influence of particle flow rate on maximum temperature in raceway zone

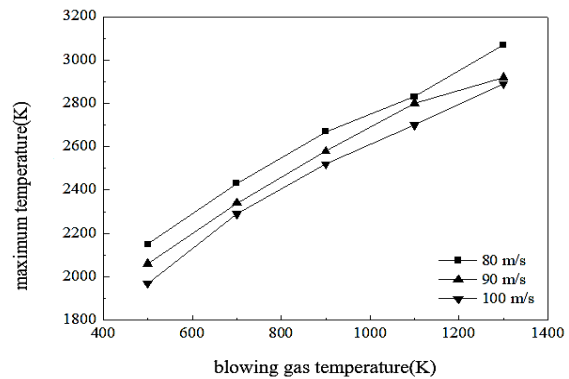


**Fig. 9** Influence of blowing gas temperature on maximum temperature in raceway zone

Fig.8 shows the effect of particle flow rate on the maximum temperature of the raceway zone under different oxygen injection rates. It can be seen from the figure that under the condition of a certain oxygen injection velocity, as the increases of flow rate of coke particles, the maximum temperature in the raceway zone also increases to 3000 K. The increase in particle flow rate indicates that the more coke particles are entrapped in the raceway, the more heat is generated by the combustion reaction of coke and oxygen in the case of sufficient oxygen, and the temperature in the raceway is also increased, as is the maximum temperature.

Another information shown in the figure is that under the same particle injection flow rate, the greater the oxygen injection rate, the smaller the maximum temperature at which the particles are burned. When oxygen enters the cavity and burns, it will absorb a part of the heat. When the particle injection rate is constant, the generated heat is basically constant. At this time, the more oxygen-enriched air is blown in, the lower the maximum temperature in the cavity will decrease.

#### **4.3. Effect of the temperature of the blowing gas on the maximum temperature of the raceway**

Under the conditions of the blowing gas velocity are 80 m/s, 90 m/s and 100m/s respectively, particle flow rate of 0.5 kg/s, particle diameter of 100  $\mu\text{m}$ , investigate the influence of wind temperature on the maximum temperature in the raceway zone, as shown in Fig. 9. It can be seen from the figure that there is a trend at different wind temperatures: as the increases of temperature of the blowing gas (wind temperature), the maximum temperature of the raceway zone rises. In the case where the flow rate of the coke particles are determined. The amount of heat generated is determined. The temperature of the oxygen entering the raceway zone from the tuyere is lower than the temperature of the cavity. After the gas enters, a part of the sensible heat is absorbed to reach the average temperature of the raceway zone. Therefore, the higher the wind temperature, the more heat is brought into the raceway zone, and the more total heat is in the raceway zone, therefore the higher the temperature in the raceway zone, the higher the maximum temperature.

## **5. Conclusions**

In this paper, the DPM model, P1 model, and porous medium boundary conditions and so on are used to simulate the combustion of coke particles in the raceway zone. The flow field, pressure field, temperature field and concentration distribution of each component in the raceway zone were analyzed. The influence of coke particle flow rate and blowing gas temperature on the maximum temperature in the raceway zone was discussed. The main results are as follows.

(1) The airflow in the raceway zone rotates and flows in the cavity along the boundary of the raceway zone, and the center of the cavity of the raceway zone presents a circular area with a relatively static airflow velocity.

(2) In the raceway area, the pressure value in the sidewall area directly opposite the direction of the air flow is the largest, and gradually decreases along the direction of the air flow, while the pressure value in the central area of the cavity is the smallest.

(3) The temperature in the cavity becomes larger and larger with the combustion of coke after the oxygen enters, and finally reaches the maximum in the upper part of the cavity region, and the maximum value is above 3 000 K.

(4) During the combustion process, the concentration of O<sub>2</sub> decreases, and the concentration of CO increases. The highest CO content in the gas leaving the raceway zone and entering the coke bed is about 0.95, while the lowest O<sub>2</sub> content is 0.05.

(5) The higher the rate of coke particle flow into the cavity from the boundary around the raceway zone, the higher the maximum temperature in the raceway zone. The higher the temperature of the tuyere blowing gas, the higher the maximum temperature of the raceway zone.

## Acknowledgements

The authors acknowledge the natural science foundation of Liaoning province (No.20170540476, No.2019-ZD-0520, and No.2019-MS-175), Liaoning province doctor startup fund (No.20170520079). And also the special thanks to the project, which is sponsored by ‘Liaoning BaiQianWan Talents Program’.

## Nomenclature

$A_p$ –particle surface are, [m <sup>2</sup> ]	$C_D$ –drag coefficient, [-]
$C_p$ –specific heat capacity, [Jkg <sup>-1</sup> °C <sup>-1</sup> ]	$d$ -diameter of particle, [-]
$H_{\text{reaction}}$ –heat generated by the surface reaction, [J]	$h$ –convection heat transfer coefficient, [Wm <sup>-2</sup> K <sup>-1</sup> ]
$f_h$ –the ratio of absorption heat of the particle, [-]	$k$ -heat transfer coefficient of the fluid, [Wm <sup>-2</sup> K <sup>-1</sup> ]
$Re$ –Reynolds number, [-]	$Y_i$ –volume concentration of $i$ , [-]
$v$ –velocity, [ms <sup>-1</sup> ]	
<i>Greek symbols</i>	
$\rho$ –density of fluid, [kgm <sup>-3</sup> ]	$\rho_p$ –density of particle, [kgm <sup>-3</sup> ]
$\varepsilon_p$ –void, [-]	$\mu$ –molar viscosity of the fluid, [Pas]
$\theta$ –radiation temperature, [K]	$\sigma$ –the steven-Boltzmann constast, [-]

## 6. References

- [1] Anameric, B., *et al.*, Direct Iron Smelting Reduction Processes, *Minerals Processing and Extractive Metallurgy Review*, 30 (2008), pp. 1-51
- [2] Qu, Y. X., *et al.*, A Comprehensive Static Model for COREX Process, *ISIJ International*, 52 (2012), 12, pp. 2186-2193
- [3] Zhou, H., *et al.*, Discrete Particle Simulation of Solid Flow in a Large-Scale Reduction Shaft Furnace with Center Gas Supply Device, *ISIJ International*, 58 (2018), 3, pp. 422-430
- [4] Kumar, P. P., *et al.*, Operating Experiences with Corex and Blast Furnace at JSW Steel Ltd, *Ironmaking & Steelmaking*, 35 (2008), 4, pp. 260-263
- [5] Zhou, H., *et al.*, Analysis of Coke Oven Gas Injection from Dome in COREX Melter Gasifier for Adjusting Dome Temperature, *Metals*, 8 (2018), 11, 921
- [6] Di, Z. X., *et al.*, Fractal Study on Raceway Boundary, *Journal of Iron and Steel Research International*, 18 (2011), 5, pp. 16-19
- [7] Gupta, G. S., *et al.*, Comparison of Blast Furnace Raceway Size with Theory, *ISIJ International*, 46 (2006), 2, pp. 195-201
- [8] Guo S. Y., Study on Simulation of BF Raceway by CFX Software, *Shandong Metallurgy*, 30 (2008), 1, pp. 56-57

- [9] Qiu J. H., Numerical Simulation of Pulverized Coal Combustion in BF Raceway Injected by Oxy-Coal Burner, *Journal of Iron and Steel Research*, 8 (1995), 1, pp. 1-5
- [10] Zhang L. L., *et al.*, Three-dimensional Modelling of Pulverized Coal Combustion Process in the Raceway of Blast Furnace, *Journal of Qingdao University (Engineering Technology Edition)*, 20 (2005), 4, pp. 44-48.
- [11] Zhang Y. P., *et al.*, Numerical Simulation of Pulverized Coal Combustion Two-Phase Flow, *Journal of Xi'an University of Science and Technology*, 28 (2008), 2, pp. 297-299
- [12] Gu M. Y., Numerical Simulation and Application of Aerodynamic Characteristics and Combustion Process of Pulverized Coal Combustion, Ph. D. thesis, Shanghai Jiaotong University, Shanghai, China, 2008
- [13] Huang D. F., *et al.*, A Comprehensive Simulation of the Raceway Formation and Combustions, *AISTech 2009 Proceedings*, 2009, I, pp. 333-344
- [14] Shen, Y. S., *et al.*, Modelling of Injecting a Ternary Coal Blend into a Model Ironmaking Blast Furnace, *Minerals Engineering*, 90 (2016), pp. 89-95
- [15] Shen, Y. S., *et al.*, Model Study of the Effect of Bird's Nest on Transport Phenomena in the Raceway of an Ironmaking Blast Furnace, *Minerals Engineering*, 63 (2014), pp. 91-99
- [16] Hou, Q. F., *et al.*, Discrete Particle Modeling of Lateral Jets into a Packed Bed and Micromechanical Analysis of the Stability of Raceways. *AIChE*, 62 (2016), 12, pp. 4240-4250
- [17] Hilton, J. E., *et al.*, Raceway Formation in Laterally Gas-driven Particle Beds, *Chemical Engineering Science*, 80 (2012), 10, pp. 306-316
- [18] Sun, J. J., *et al.*, Numerical Simulation of Raceway Phenomena in a COREX Melter Gasifier, *Powder Technology*, 281 (2015), pp. 159-166
- [19] Wei G. C., *et al.*, CFD-DEM Study on Heat Transfer Characteristics and Microstructure of the Blast Furnace Raceway with Ellipsoidal Particles, *Powder Technology*, 346 (2019), pp. 350-362
- [20] Miao Z., *et al.*, CFD-DEM Simulation of Raceway Formation in an Ironmaking Blast Furnace, *Powder Technology*, 314 (2017), pp. 542-549